IL NUOVO CIMENTO **44 C** (2021) 7
DOI 10.1393/ncc/i2021-21007-8

COMMUNICATIONS: SIF Congress 2020

Spin-to-charge conversion in Bi_2Se_3/Ge(111)

ADELE MARCHIONNI
LNESS-Dipartimento di Fisica, Politecnico di Milano - Milano, Italy

received 26 January 2021

Summary. — Nowadays, topological insulators (TIs) are receiving an increasing attention. This is due to the fact that these materials exhibit spin-polarized surface states, which can be exploited to convert a spin current into a charge current and vice versa. Here, we investigate a prototypical TI/semiconductor system: a patterned Bi_2Se_3/Ge(111) heterostructure, where spin-polarized electrons are injected inside Ge by means of optical orientation and detected in a Bi_2Se_3 bar, after diffusion in the Ge substrate. The spin current is converted into a measurable electric potential by means of the inverse Rashba-Edelstein effect (IREE). We employ a non-local injection-detection scheme, since spin generation and detection are spatially separated. We have studied the IREE signal as a function of the degree of circular polarization and power of the light. Moreover, we estimate the value of the spin-diffusion length in Ge(111) which is $l_s \approx 5.8$ μm, in agreement with previous literature reports. We thus conclude that the Bi_2Se_3/Ge(111) can be effectively exploited as a reliable spin detector.

1. – Introduction

Topological insulators (TIs) are receiving an increasing interest, since theorethical studies suggest that an efficient 2D spin-charge interconversion can be obtained at their surface [1]. This is due to the fact that TIs show spin-momentum locked surface states [2], which allow for the conversion of a spin accumulation into a charge flow and vice versa [3-7]. The former process is already employed to detect spin-polarized electron populations [8]. Moreover, the presence of spin-momentum locked surface states produces promising unidirectional magnetoresistance terms [9]. Spins are commonly injected inside TIs by means of spin pumping [10, 11]. This technique, however, requires the use of ferromagnets [10], which could trigger undesired chemical reactions with TIs, drastically moidfying the TI surface properties [12, 13]. To circumvert this issue, it is possible to grow TIs on semiconductor substrates [14]. In TI/semiconductor heterojunctions, indeed, the TI interface state topology is almost preserved [8] and spin injection can be performed by means of the optical orientation technique [8] by photogenerating a spin-polarized electron population in the conduction band of the semiconductor, as a

consequence of the absorption of circularly polarized light [15-18]. Moreover, an efficient spin-to-charge conversion occurring in materials grown on top of the semiconductor has already been documented [19, 8] and these heterostructures allow addressing fundamental spin-related transport properties, such as the spin-diffusion length [20-25]. Among semiconductors, Ge is an ideal platform to inject spins [26], since the spin polarization, at the generation time, is as high as 50% when the photon energy is tuned to the Ge direct gap [27]. This material also represents a suitable platform for spin transport thanks to the reported large values of the spin diffusion length [20, 21]. Moreover, the integration of spintronic devices with either electronic or photonic ones is promoted by the high compatibility between Ge and Si, due to a lattice mismatch of 4% [28], and by the Ge energy gap matching the telecommunication window [29].

Here, we investigate the spin-to-charge conversion occurring in a prototypical TI/semiconductor system, namely Bi_2Se_3/Ge(111). In-plane spin-polarized electrons are optically oriented inside Ge, below the edges of Pt stripes patterned on the Ge(111) surface [26, 21]. Spin-polarized electrons diffuse in the substrate and reach the Bi_2Se_3 pad, where they undergo spin sorting. In [8] we show that the resulting spin-to-charge conversion is related to the inverse Rashba-Edelstein effect (IREE) [30, 31], occurring in hybridized interface states between the Bi_2Se_3 and Ge(111). The resulting charge accumulation is detected in open-circuit condition as a voltage drop ΔV between two electrodes placed at opposite sides of the Bi_2Se_3 pad. This injection-detection scheme is a non-local process, since spin-polarized electrons are excited in one point of the sample and they are detected in a different one.

In this work, we report the IREE signal of the Bi_2Se_3 heterojunction, we characterize it as a function of the DCP and the incident power and we show how these experimental results can be used to estimate the spin-diffusion length in Ge.

2. – Methods

The investigated system is represented in fig. 1(a): it is composed by a 2 μm-thick n-doped Ge(111) substrate with dopants concentration $N_d = 9 \times 10^{16}$ cm^{-3}, grown on top of a semi-insulating Si platform. A set of Pt stripes and a Bi_2Se_3 bar are lithographically defined on the Ge surface. Further growth and fabrication details can be found in ref. [8]. The Pt stripes are 20×2 μm^2 large and 15 nm-thick, while the Bi_2Se_3 detector has an area of 75×20 μm^2 and a thickness of 10 nm. The center-to-center separation between one stripe and the next one is ≈ 10 μm, along the x-direction in the reference frame of fig. 1(a). The Bi_2Se_3 stripe is contacted at both ends by Au-Ti pads, deposited over 80 nm of SiO_2 to avoid direct spin absorption from the electrodes.

The experimental setup is sketched in fig. 1(b). We employ the monochromatized beam (1550 nm) of a supercontinuum laser (NKT Photonics, SuperK Extreme EXW-12) as a light source([1]). We exploit a photo-elastic modulator (PEM) to modulate the circular polarization of the light at 50 kHz. The laser beam is focused on the sample surface by a 60× objective (numerical aperture = 0.7), resulting in a spot diameter on the sample of ≈ 3 μm. When the focused light beam impinges on the edge of a Pt stripe, the metal pattern produces an elliptic component of the electromagnetic wave in the xz-plane [26].

([1]) The laser repetition rate is 78 MHz, with nanosecond-duration pulses. The analyzed data are time-averaged. Note that the time-averaged solution of the time-dependent drift-diffusion equation results to be the same as the steady-state solution [32]. Therefore, the laser temporal structure can be safely neglected in our analysis.

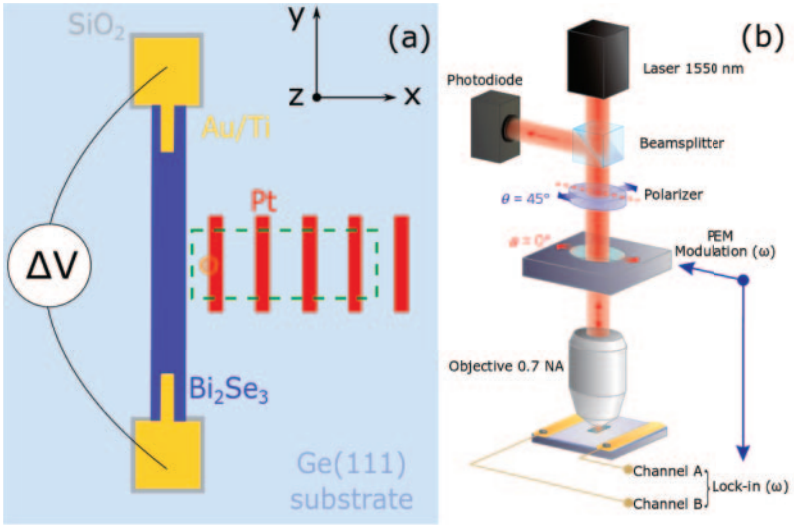

Fig. 1. – (a) Schematic structure of the investigated sample: Pt stripes (red) are exploited for spin injection, while a Bi_2Se_3 pad is exploited as spin detector (blue). The two Au-Ti electrodes (yellow) are insulated from the substrate by a SiO_2 layer (gray). The dashed green region is where the data of fig. 2 are acquired. The orange circle is the point where the laser beam is focused for the acquisition of fig. 3. Panel (b) shows the experimental setup based on a confocal microscope. A 1550 nm light from a supercontinuum laser is employed as a light source. The circular polarization of the light beam is modulated by a photoelastic modulator (PEM). The spin-to-charge conversion signal ΔV acquired across the Bi_2Se_3 stripe is demodulated at the PEM frequency (50 kHz) by a lock-in amplifier.

According to the optical orientation principles [15-17], this component photoexcites an electron population with a spin polarization along the x-axis [26, 21], localized below the edge of the Pt stripe in Ge. If the light illuminates the opposite edge of the Pt stripe, the spin polarization is reversed [26]. After the generation, spins diffuse in the Ge substrate until they enter the Bi_2Se_3 pad. We showed in ref. [8] that the spin current is converted into a charge current by means of the IREE occurring in the interface states of Bi_2Se_3/Ge(111). Since the electrodes can only measure a charge current directed along the y-axis (reference frame of fig. 1(a)), only electrons with a spin polarization along x can be detected (see [33] for the IREE geometry). We record the voltage drop across the detector while raster scanning the sample surface with the focused light beam. The signal is then demodulated by a lock-in amplifier at the PEM frequency (50 kHz). Together with the electric signal, we record the point-by-point reflectivity map of the sample with a photodiode detector. All the measurements are performed at room temperature.

3. – Results and discussion

In fig. 2(a), (b), we report the reflectivity and IREE map, respectively, resulting from the raster scanning procedure explained in sect. 2. These maps are obtained with an impinging light power $P = 18\ \mu$W and DCP = 100% (see the following section). By averaging, along the y-axis (reference frame of fig. 1(a)), the maps of fig. 2(a), (b), we obtain the optical (red) and IREE (blue) profiles shown in fig. 2(c). These data show that the IREE voltage drop is reversed at the opposite edges of the Pt stripes, as a first confirmation of a spin dependence of the IREE signal.

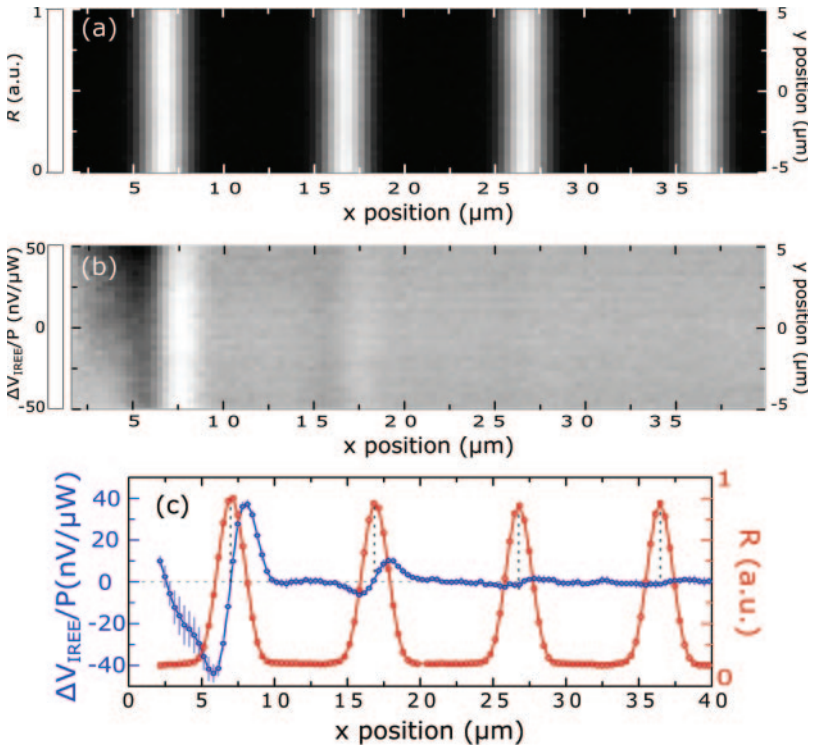

Fig. 2. – Optical (a) and IREE map (b) and the optical (red) and IREE (blue) averaged profiles (c). The error bars in (c) account for the fluctuation of the data, being twice their standard deviation. These maps and profiles are acquired with $h\nu = 0.8\,\text{eV}$, $P = 18\,\mu\text{W}$ and DCP = 100%. Data are normalized to the impinging power.

3˙1. *Preliminary checks*. – To check the spin-related nature of the measured IREE signal, we investigate the dependence of ΔV, as a function of the degree of circular polarization (DCP) and of the power of the impinging light beam (P). Indeed, an electric signal produced by optically oriented spins should be linearly dependent on both quantities [17].

The DCP can be experimentally tuned by changing the PEM phase delay $\Delta\phi$ [19]. In terms of Stokes parameters, the light circular polarization is described by the σ_4 parameter, which is

$$\sigma_4 = \sin[\Delta\phi\,\cos(2\pi\, f\, t)], \tag{1}$$

where t is time and f the PEM frequency. Since we demodulate the first harmonic of the electric signal with the lock-in amplifier, we can expand (1) in Fourier series and consider just the f-dependent term, which is

$$\sigma_4^f = 2J_1(\Delta\phi), \tag{2}$$

being J_1 the first Bessel function. A convenient definition of the DCP is

$$\text{DCP} = \sigma_4^f / \sigma_{4,max}^f, \tag{3}$$

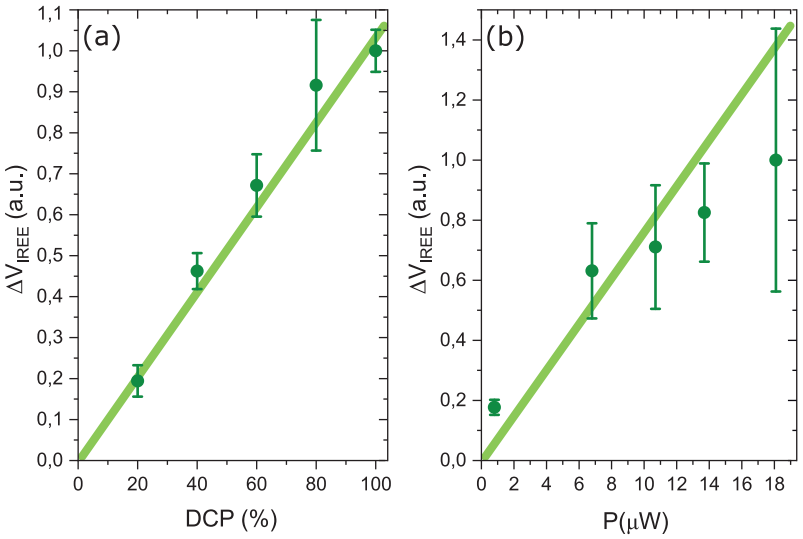

Fig. 3. – Dependence of the IREE signal as a function of the degree of circular polarization (a) and power (b) of the impinging light beam. Data are acquired with the laser spot focused on the orange circle of fig. 1(a). Data in panel (a) are acquired at $P = 18$ μW, data in panel (b) are acquired at DCP = 100%. The error bars account for the fluctuation of the data, being twice their standard deviation.

where $\sigma^f_{4,\max}$ is the maximum value of σ^f_4, corresponding to $\Delta\phi \approx 0.3\,\lambda$. The experimental results, obtained when the light beam is focused on the first Pt stripe near the detector (orange circle in fig. 1(a)), are reported in fig. 3(a). The detected signal is linearly dependent on the DCP [34].

The dependence upon the laser power is acquired with the laser spot focused in the same point where the DCP dependence has been recorded (orange circle in fig. 1(a)). The results are shown in fig. 3(b) and a linear trend, within the experimental error, is confirmed also in this case. These measurements confirm the spin-related nature of the detected signal.

3˙2. *Spin diffusion length.* – From fig. 2 we observe that spins generated closer to the detector produce a larger signal than the ones generated farther. This can be better appreciated in fig. 4, where we report the absolute value of the IREE peaks at each edge of the Pt stripes (data taken from the IREE profile in fig. 2(c)). The decay is due to the depolarization occurring to spins during the diffusion in the Ge substrate from the generation to the detection points [14, 35]. The depolarization can be modelled considering the proportionality between the measured ΔV and the spin current reaching the detector position i_s.

This decay can be fitted with a one-dimensional diffusion model, as reported in [36-38, 24]. In fact, the resulting spin current at the detector position can be described by an exponential decay having the following form:

$$i_s(x) = i_{s,0}\, e^{-\frac{x}{l_s}}, \tag{4}$$

being $i_{s,0}$ the spin current injected at the generation time, x the distance between the spin detector and the point where spins are optically generated, and l_s the electron spin-

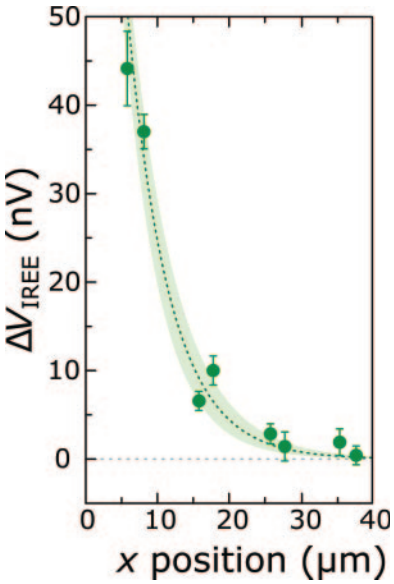

Fig. 4. – The dark green points are the absolute value of the IREE signal acquired at each edge of the Pt stripes (data from fig. 2(c) – blue data). The error bars account for the fluctuation of the data, being twice their standard deviation. The light green band shows the best fit (with its error) of the data with a 1D exponential decay.

diffusion length of Ge(111). Analytical calulations can be found in [37]. The best fit of the data in fig. 4 with the 1D diffusion model of (4) gives a spin-diffusion length of $l_s = 5.8 \pm 0.7$ μm in Ge(111), comparable with previous literature results [20, 21, 39].

4. – Conclusions

We have investigated the spin-to-charge conversion in a Bi_2Se_3/Ge(111) system. We have employed optical orientation to generate a spin population by expoiting circularly polarized light, while the electrical detection is performed in a Bi_2Se_3 bar. This injection-detection process allows avoiding the use of ferromagnets, which could chemically alter the spin-polarized surface states, denaturing the peculiarity of TIs. We have examined the Bi_2Se_3 IREE signal dependence upon the DCP and the impinging power, observing a linear dependence on both parameters, which confirms the spin nature of the IREE signal. Moreover, we have addressed the value of the spin diffusion length in Ge(111) which results to be $l_s \approx 5.8$ μm. Our analysis confirms that the Bi_2Se_3/Ge(111) interface can be safely employed as a reliable ultra-thin spin detector.

* * *

The author would like to acknowledge T. Guillet, C. Zucchetti, A. Hallal, P. Biagioni, C. Vergnaud, A. Marty, H. Okuno, A. Masseboeuf, M. Finazzi, F. Ciccacci, M. Chshiev, F. Bottegoni and M. Jamet for collaborating in the presented work.

REFERENCES

[1] Shi S., Wang A., Wang Y., Ramaswamy R., Shen L., Moon J., Zhu D., Yu J., Oh S., Feng Y. and Yang H., *Phys. Rev. B*, **97** (2018) 041115.
[2] Hasan M. Z. and Kane C. L., *Rev. Mod. Phys.*, **82** (2010) 3045.
[3] Edelstein V. M., *Solid State Commun.*, **73** (1990) 233.
[4] Geng H., Luo W., Deng W. Y., Sheng L., Shen R. and Xing D. Y., *Sci. Rep.*, **7** (2017) 1.
[5] Chen W., *J. Phys. Condens. Matter*, **32** (2019) 035809.
[6] Bottegoni F., Calloni A., Bussetti G., Camera A., Zucchetti C., Finazzi M., Duò L. and Ciccacci F., *J. Phys. Condens. Matter*, **28** (2016) 195001.
[7] Zucchetti C., Dau M.-T., Bottegoni F., Vergnaud C., Guillet T., Marty A., Beigné C., Gambarelli S., Picone A., Calloni A., Bussetti G., Brambilla A., Duò L., Ciccacci F., Das P. K., Fujii J., Vobornik I., Finazzi M. and Jamet M., *Phys. Rev. B*, **98** (2018) 184418.
[8] Guillet T., Zucchetti C., Marchionni A., Hallal A., Biagioni P., Vergnaud C., Marty A., Okuno H., Masseboeuf A., Finazzi M., Ciccacci F., Chshiev M., Bottegoni F. and Jamet M., *Phys. Rev. B*, **101** (2020) 184406.
[9] He, P., Zhang, S. S.-L., Zhu, D., Liu, Y., Wang, Y., Yu, J., Vignale, G. and Yang, H., *Nat. Phys.*, **14** (2018) 495.
[10] Takahashi S., *Physical Principles of Spin Pumping*, in *Handbook of Spintronics*, edited by Xu Y., Awschalom D. and Nitta J. (Springer, Dordrecht) 2016.
[11] Brataas A., Tserkovnyak Y. and Bauer G. E., *J. Magn. & Magn. Mater.*, **272-276** (2004) 1981.
[12] Walsh L. A., Smyth C. M., Barton A. T., Wang Q., Che Z., Yue R., Kim J., Kim M. J., Wallace R. M. and Hinkle C. L., *J. Phys. Chem. C*, **121** (2017) 23551.
[13] Ferfolja K., Valant M., Mikulska I., Gardonio S. and Fanetti M., *J. Phys. Chem. C*, **122** (2018) 9980.
[14] Dyakonov M., *Spin Physics in Semiconductors*, Vol. **1** (Springer-Verlag) 2008.
[15] Meier F. and Zakharchenya B. P., *Optical Orientation* (Elsevier) 1984.
[16] Lampel G., *Phys. Rev. Lett.*, **20** (1968) 491.
[17] Dyakonov M. and Perel V., *Mod. Prob. Condens. Matter Sci.*, **8** (1984) 11, 15.
[18] Bottegoni F., Ferrari A., Rortais F., Vergnaud C., Marty A., Isella G., Finazzi M., Jamet M. and Ciccacci F., *Phys. Rev. B*, **92** (2015) 214403.
[19] Zucchetti C., Ballabio A., Chrastina D., Cecchi S., Finazzi M., Virgilio M., Isella G. and Bottegoni F., *Phys. Rev. B*, **101** (2020) 115408.
[20] Zucchetti C., Bollani M., Isella G., Zani M., Finazzi M. and Bottegoni F., *APL Mater.*, **7** (2019) 101122.
[21] Zucchetti C., Bottegoni F., Vergnaud C., Ciccacci F., Isella G., Ghirardini L., Celebrano M., Rortais F., Ferrari A., Marty A., Finazzi M. and Jamet M., *Phys. Rev. B*, **96** (2017) 014403.
[22] Bottegoni F., Zucchetti C., Ciccacci F., Finazzi M. and Isella G., *Appl. Phys. Lett.*, **110** (2017) 042403.
[23] Bottegoni F., Zucchetti C., Isella G., Pinotti E., Finazzi M. and Ciccacci F., *J. Appl. Phys.*, **124** (2018) 033902.
[24] Bottegoni F., Zucchetti C., Isella G., Bollani M., Finazzi M. and Ciccacci F., *Riv. Nuovo Cimento*, **43** (2020) 45.
[25] Bottegoni F., Ferrari A., Isella G., Finazzi M. and Ciccacci F., *Phys. Rev. B*, **85** (2012) 245312.
[26] Bottegoni F., Celebrano M., Bollani M., Biagioni P., Isella G., Ciccacci F. and Finazzi M., *Nat. Mater.*, **13** (2014) 790.
[27] Rioux J. and Sipe J. E., *Phys. Rev. B*, **81** (2010) 155215.
[28] Haddara Y. M., Ashburn P. and Bagnall D. M., *Mater. Today*, **10** (2006) 55.
[29] Hochberg M. and Baehr-Jones T., *Nat. Photon.*, **4** (2010) 492.

[30] Wang H., Kally J., Lee J. S., Liu T., Chang H., Hickey D. R., Mkhoyan K. A., Wu M., Richardella A. and Samarth N., *Phys. Rev. Lett.*, **117** (2016) 076601.
[31] Matsushima M., Ando Y., Dushenko S., Ohshima R., Kumamoto R., Shinjo T. and Shiraishi M., *Appl. Phys. Lett.*, **110** (2017) 1.
[32] Zucchetti C., Isella G., Ciccacci F., Finazzi M. and Bottegoni F., *Spin transport and spin-charge interconversion phenomena in Ge-based structures*, in *Proceedings of Spintronics XII*, edited by Drouhin H.-J. M., Wegrowe J.-E. and Razeghi M., Vol. 11090 (SPIE) 2019, pp. 73–82.
[33] Gambardella P. and Miron I. M., *Philos. Trans. R. Soc. A*, **369** (2011) 3175.
[34] Ando K., Morikawa M., Trypiniotis T., Fujikawa Y., Barnes C. H. W. and Saitoh E., *J. Appl. Phys.*, **107** (2010) 113902.
[35] Zucchetti C., Bottegoni F., Isella G., Finazzi M., Rortais F., Vergnaud C., Widiez J., Jamet M. and Ciccacci F., *Phys. Rev. B*, **97** (2018) 125203.
[36] Zutić I., Fabian J. and Das Sarma S., *Rev. Mod. Phys.*, **76** (2004) 323.
[37] Fabian J., Matos-Abiaguea A., Ertlera C., Stano P. and Zutić I., *Acta Phys. Slovaca*, **57** (2007) 565.
[38] Spiesser A., Saito H., Fujita Y., Yamada S., Hamaya K., Yuasa S. and Jansen R., *Phys. Rev. Appl.*, **8** (2017) 1.
[39] Rinaldi C., Bertoli S., Asa M., Baldrati L., Manzoni C., Marangoni M., Cerullo G., Bianchi M., Sordan R., Bertacco R. and Cantoni M., *J. Phys. D: Appl. Phys.*, **49** (2016) 425104.